FEATURES OF HEAT TRANSFER AT INTERACTION OF AN IMPACT SWIRL JET WITH A DIMPLE

by

Viktor I. TEREKHOV * ***and Yuriy M. MSHVIDOBADZE***

Kutateladze Institute of Thermophysics, Siberian Branch of the Russian Academy of Sciences, Novosibirsk, Russia

Original scientific paper
DOI: 10.2298/TSCI150819137T

Experimental results on investigation of heat transfer at interaction of an air impact jet with a semi-spherical cavity are presented in this work. This research is continuation of investigations of turbulent jet interaction with complex surfaces and search for the method of heat transfer control. Experiments were carried out with fixed geometry of a semi-spherical cavity (D_C = 46 mm) and swirl parameter (R = 0; 0.58; 1.0; 2.74). The distance between the axisymmetric nozzle and obstacle was 2-10 sizes over the nozzle diameter, and the Reynolds number, Re_0, varied within 1 to $6\cdot10^4$. It was found out that with an increase in swirling heat transfer intensity decreases due to fast mixing of the jet with ambient medium. In general, the pattern of swirl jet interaction with a concave surface is complex and multifactor.

Key words: *impinging jet, swirl number, dimple, heat transfer, control, turbulent regime*

Introduction

Jets impinging onto heat-exchanging surfaces can be used in many technical apparatuses as very efficient heat-transfer intensifiers. Interest in this field was initiated many years ago, and since then ample data concerning this problem have been accumulated [1, 2]. Nonetheless, jets of interest still attract considerable attention, and extensive studies aimed at searching for new methods to control heat and mass transfer in such systems are presently under way. One strategy here implies modification of the surface onto which the jets impinge with obstacles. The authors of [3-5] examined heat transfer in narrow channels in which a system of jets impinging onto a surface modified with cavities was organized. It was shown that such systems exhibit good performance characteristics and can be used, in particular, for cooling turbine blades from inside. Yet, the physical reasons underlying the observed intensification of heat-transfer processes in the systems of interest have remained unveiled.

The detailed structure of the flow and heat transfer during the interaction of an impinging jet with a single hole was studied in experimental works [6-10]. In [11-16], the problem of jet penetration into the cylindrical cavities, extended along the length, is considered. Widespread practical application of the impinging jets caused numerous studies of complex interactions of the single jets and their systems with the surfaces of various shapes [17, 18]. The cases of in leakage of high-temperature jets and flames on the surface [19-21], when the craters of approximately spherical shape are formed there, are of a particular importance.

Cavities used as obstacles modifying the streamlined surfaces attract considerable interest as they proved capable of generating exotic self-oscillatory flow modes and intensify-

* Corresponding author; e-mail: terekhov@itp.nsc.ru

ing heat transfer [22-25]. In the case of jets impinging onto heat-exchanging surfaces the interaction pattern of the jet flow with the surface is much more complicated compared to a flat surface. For instance, vortex formation processes and local flow separations induced by obstacles prepared in the form of cavities may give rise to a complex, unstable flow involving large-scale low-frequency oscillations, Taylor-Gortler vortices, *etc.* Under such conditions, accurate prediction of heat-transfer processes becomes problematic, although this problem was addressed in several publications.

The aerodynamic structure of the flow and the heat transfer from hemispherical cavity *vs.* the jet Reynolds number and as functions of the distance from the nozzle exit to the heat-exchanging surface were examined in [6, 7]. The jet flow was not swirling, and the cavity-to-nozzle diameter ratio was $D_c/d_0 = 5.4$. The average heat transfer from the cavity surface was found to be decreased twice compared to the case of a flat surface, all other conditions being identical. With decreasing the nozzle diameter, the heat transfer grows in value and, according to [9], at $D_c/d_0 = 44$ its intensity may become exceeding the same quantity for flat surface. Moreover, in the region outside the cavity the thermal interaction between the lateral flow and the jet rapidly degenerates, making the heat transfer almost vanishing here [7]. In the cavity, pronounced vortex formations arise. These formations, resembling Taylor-Gortler vortices, give rise to coherent structures that can be easily registered by heat flow microsensors.

In [10], local heat transfer in hemispherical cavity was examined as a function of cavity-to-nozzle diameter ratio in the range $D_c/d_0 = 11$-30. Here, unlike in [9], increase in the nozzle diameter was found to suppress heat transfer throughout the whole examined range of Reynolds numbers, $\mathrm{Re}_0 \sim 10^4$ to $5 \cdot 10^4$. Thus, the experimental data concerning the interaction of jet flows with curvilinear surfaces are still few in number and contradictory.

The problem becomes even more complicated if the jet flow impinging onto an obstacle has a rotational velocity component. So far, the heat transfer and the structure of flow between a swirling jet and a surface onto which this jet impinges remain poorly understood. Reported studies [26-40], also few in number, show the interaction of a swirling jet with an obstacle to be a complex many-factor process. An increase in jet pre-rotation intensity enhances mixing processes in the system. As a result, the heat transfer of the surface interacting with the jet at large nozzle-to-surface separations ($L/d_0 > 6$) turns out to be substantially reduced in comparison with non-swirling jets. At small nozzle-to-surface separations, $L/d_0 < 6$, the picture may be opposite, with additional maxima emerging in the radial distribution of heat-transfer intensity due to specific formation pattern of swirling jets with different pre-rotations, Reynolds numbers, and separations between the jet turning point and the surface onto which the jet impinges.

Expectedly, pre-rotation of the jet approaching a surface modified with a spherical cavity will complicate the problem. The fluid leaving the cavity will interact with the rotational jet flow impinging onto the obstacle, thus causing the formation of unsteady 3-D flows hard to predict numerically. Firstly, it was shown in the experimental works of [41, 42], and the current study is a continuation of this research.

The purpose of the present study was to experimentally examine the time-average heat transfer from a surface with spherical cavity during impingement of a swirling jet onto this surface. Such flows are often encountered in low-temperature plasma generators and in power-plant cooling systems.

Experimental set-up and measurements

The experiments were carried out on an experimental set-up, whose schematic diagram is shown in fig. 1. This set-up was described in detail elsewhere [43]. A room-temperature axisymmetric swirling air jet emanated out of the nozzle whose diameter was d_0 = 8.9 mm. The cavity diameter was fixed, equal to D_c = 46 mm (D_c/d_0 = 5.17), and the cavity depth was either Δ = 0, 12, or 23 mm. The gas-flow velocity U_0 at the nozzle exit plane was varied in the range from 20-100 m/s, corresponding to, $\mathrm{Re}_0 = U_0 d_0/\nu = 10^4\text{-}5\cdot10^4$.

The distribution of flow velocity over the nozzle outlet was almost uniform, the turbulence number being $Tu \cong 0.3\%$. This was achieved due to the strong acceleration of the flow in a shaped nozzle with the contraction ratio of ~32 as well as installation of the leveling grids. The jet approached the obstacle normally, and the nozzle-to-surface separation S was varied from 0-10 d_0.

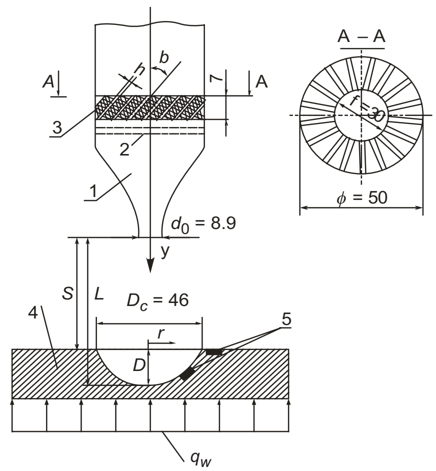

Figure 1. Experimental set-up; *1 – nozzle, 2 – honeycombs, 3 – swirler, 4 – cupper obstacle, 5 – heat-flux meters*

The jet flow was made swirling by pre-rotating it with a flat swirler with variable slit inclination angle. The appearances of four swirlers are shown in fig. 2, and their geometric characteristics are presented in tab. 1. The number of slots n, through which the swirl flow was formed, differed, and the height, including that for not-swirl jet (β = 0) remained the same. Thus, the swirl parameter varied in a wide range from weak to very intense.

Figure 2. Photo of swirler for impinging jet

The jet pre-rotation parameter, defined as the momentum ratio between the circumferential component of the jet flow and the jet flow along the jet axis, was R = 0, 0.58, 1.0, and 2.74.

Table 1. Geometric characteristics of swirlers

N	h, [mm]	β, [°]	n	R
1	2.2	0	29	0.0
2	2.2	20	27	0.58
3	2.2	45	20	1.0
4	2.2	60	10	2.74

The test section, 50 mm thick and 190 mm in diameter, was prepared from copper. The desired temperature difference between the jet and the obstacle, about 40° in the majority of tests, was achieved with the help of an ohmic heater installed over the obstacle. The choice of copper, having a high value of thermal conductivity, as the obstacle material was motivated by the desire to organize the boundary condition $T_w \cong$ constant at the obstacle surface. The temperature of the streamlined surface and the flow temperature were measured by chromel-copel thermocouples.

The heat fluxes were measured by gradient-type heat flow sensors glued onto the obstacle [44]. The characteristics of the sensors were: in-plane dimensions – 2.5 mm × 2.5 mm (these dimensions were much smaller than the characteristic spatial scale of the flow under study), thickness – 0.2 mm, volt-watt sensitivity ≈ 10 mV/W, response time – 0.05 ms. In the course of measurements, the arrays of instantaneous values of heat-flux densities were used to calculate the time-average heat fluxes, and also the heat-flow pulsations and spectra. The total number of realizations in one measurement was chosen to equal 10^4. The time in which one measurement was taken was varied from 10-90 s. It was found experimentally that this time affected measured data insignificantly. A tailored multichannel unit was used to amplify the signals from the thermocouples and heat-flow sensors; then, the signals were fed to a computer to be processed there. The coefficient of heat transfer was defined:

$$\alpha_i = \frac{q_i - \Delta q_i}{T_w - T_0} \tag{1}$$

where q_i is the local heat-flux density measured by sensor, Δq_i – the heat losses by radiation and free convection, which experimentally determined and were taken into account in processing of the experimental data. T_w and T_0 are the temperature of the surface and the temperature of the air at the nozzle exit, respectively. An error analysis showed that the measurement inaccuracy for heat fluxes in our experiments was within 0.3-10%. Simultaneously, the measurement inaccuracy for square-mean pulsations of heat fluxes was much greater, amounting to 30% for the obstacle with cavity.

Local Nusselt number was determinate on the nozzle diameter and coefficient of heat conductivity on average temperature between gas and a surface under the next formula:

$$\mathrm{Nu}_i = \frac{\alpha_i d_0}{\lambda} \tag{2}$$

In the assumption axially symmetric problem, average on a dimple surface heat transfer coefficient and corresponding Nusselt number calculated:

$$\bar{\alpha} = \frac{\int_0^1 \alpha_i \bar{r} \mathrm{d}\bar{r}}{2}, \qquad \overline{\mathrm{Nu}}_D = \frac{\bar{\alpha} D_c}{\lambda} \tag{3}$$

where $\bar{r} = 2r/D_c$ is the relative radius.

Normally to the cavity surface and to the flat surface adjacent to the cavity, holes 0.5 mm in diameter were drilled, and these holes were used to measure the radial distributions of pressure. In the tests, the average component of pressure was registered, and estimates of the intensity of pressure pulsations were made.

To diagnose the vortex flow, it was used the two-component laser-Doppler system LAD-0.5M (produced at the Institute of Thermophysics), operating in the back scattering mode. In experiments, the measuring system was moved with the help of 3-D co-ordinate device with an accuracy of 5 μm. To obtain the averaged values of velocity, there were, at least, 10^4 measurements.

Interaction of an impinging jet with a flat plate

At the first stage of the study, we experimentally examined the pressure distribution and heat transfer of flat obstacles interacting with swirling jets. The value of the pressure coefficient was found as the pressure drop between the surface and the atmosphere normalized to the dynamic pressure of the jet flow at the nozzle exit plane, $c_p = 2(p_i - p_a)/\rho_0 u_0^2$.

Distribution of pressure over a flat surface without jet swirl is shown in fig. 3. It can be seen that at small distances between the nozzle and surface $S/d_0 < 4$, the pressure at the stagnation point is restored almost completely ($c_p \rightarrow 1$) and with an increasing distance between the nozzle and obstacle, the pressure coefficient decreases gradually. At short distances from the obstacles, there is an annular region of the negative pressure caused by the presence of large-scale structures and formation of a radial flow.

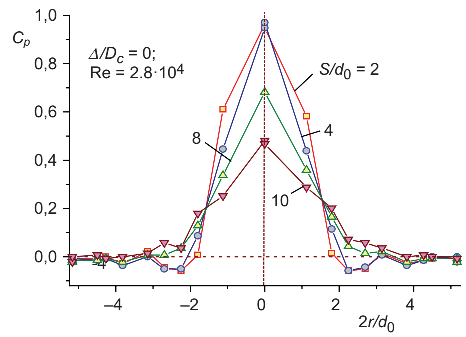

Figure 3. Pressure distribution on a flat plate for impinging jet without swirling

A specific feature of such jets is their high ejective capacity due to which the jet divergence angle grew in value with increasing jet pre-rotation [27-29]. As a result, the heat-transfer maximum got displaced off the center (fig. 4). Depending on pre-rotation and nozzle-to-obstacle separation, this maximum could be either distinctly pronounced, fig. 4(a), $L/d_0 = 2$, or smooth, fig. 4(b), $L/d_0 = 10$). A similar tendency was also observed at other jet pre-rotations. In fig. 5, were shown experimental data of effect swirling intensity on heat transfer coefficient distribution. It is visible, that with increase swirling parameter of a jets intensity of heat transfer is considerably reduced. At large parameter ($R = 2.74$) external region of flow heat transfer practically is absent, that speaks about intensive mixing impinging jets with an environment media. Importantly, in the majority of our experiments the radial distributions of local heat transfer behaved similarly, the heat transfer increasing with increasing the Reynolds number, fig. 4(a).

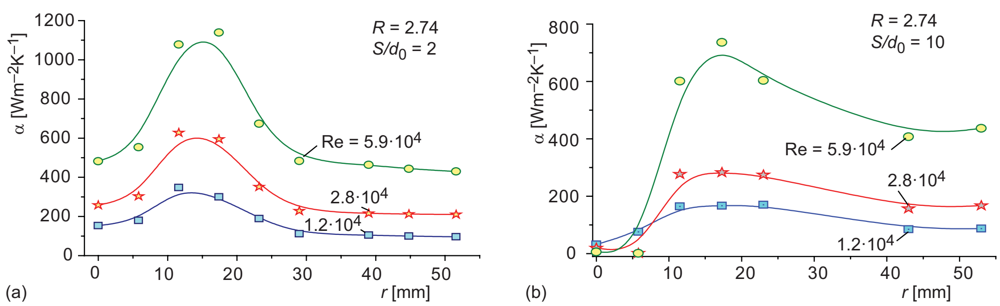

Figure 4. Distributions of heat-transfer coefficients over the flat surface interacting with a swirling jet

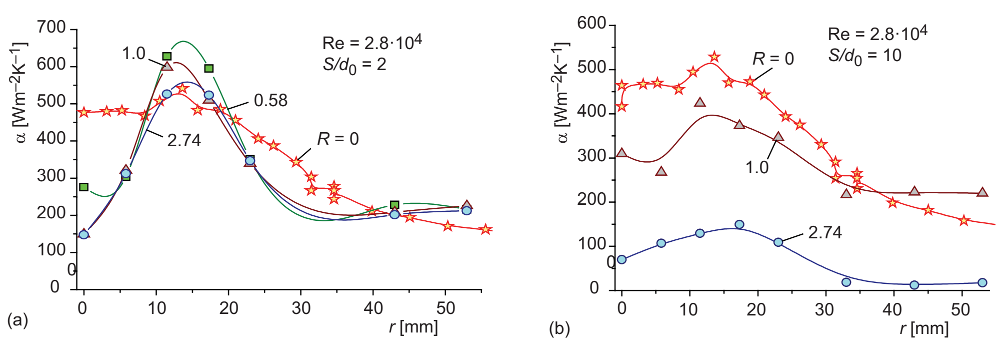

Figure 5. Effect of a swirl number on heat transfer coefficient distribution

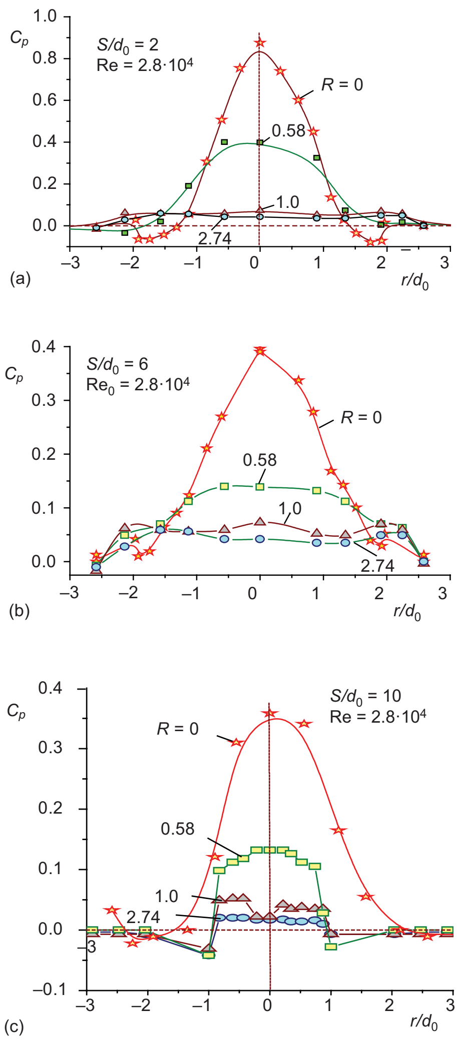

Figure 6. Pressure coefficient in the cavity onto which a swirling jet impinges; Re = 2.8·10^4; (a) S/d_0 = 2, (b) S/d_0 = 6, (c) S/d_0 = 10

Interaction of a swirling jet with a dimple. Pressure pattern and velocity profiles

A typical distribution of pressure coefficient over the radius of spherical cavity is exemplified in fig. 6. Without pre-rotation (R = 0) the pressure profile exhibits a distinct axial maximum. At the periphery, an inflection point brought about by the separation of the flow in this region is observed. The mechanism underlying the formation of flow in a cavity impinged by non-swirling jet was discussed in more detail in [6, 7].

With increasing the jet pre-rotation parameter, the pressure level notably diminished due to the rapid expansion of the jet flow and the reduction of the jet momentum in the axial region. For instance, at R = 2.74 the pressure coefficient is one order of magnitude smaller in comparison with non-swirling jet. The effect of swirl is especially strong at the large distance between the jet and obstacle, figs. 6(b) and 6(c) for S/d_0 = 6 and 10, respectively.

Another characteristic feature in the behavior of cavity pressure deserves mention. With swirling jets, the distributions of pressure in the peripheral region display no inflections. Moreover, a growth of pressure is observed in this zone due to the absence of flow separation and the action of centrifugal forces pressurizing the fluid here, as well as due to the influence of the surface curvature. Apparently, these factors will have influence on the formation of the temperature field in the system and on the heat- and mass-transfer processes proceeding there.

The important part of this work concerns experimental study of turbulent structure of the flow and turbulent fluctuations at swirl jet impinging on a surface with hemispherical cavity.

Experimental data show extreme complexity of flow formation pattern in a swirl impinging jet interacting with a spherical cavity. Due to centrifugal forces the vortex jets expand faster, and the longitudinal component of velocity decreases with an increase in the swirl parameter. As an example, fig. 7 demonstrates distribution of longitudinal component of velocity in the impinging jet at variations of initial swirl angle in a plane located 5 mm away from an obstacle. With no swirl the jet penetrates into the cavity, turns around by 180° and pools out along the lateral surface. This reverse flow mixes with the falling jet and practically does not interact with the flat surface surrounding the cavity. At that in peripheral part of the back-flow jet we observed large-scale flow fluctuations which caused strong irregularities in velocity profiles.

For swirling jets, the backflows are expressed in a much less degree and the impinging jet area stretches far beyond the cavity, what leads to heat transfer enhancement in this area. The velocity value on a jet axis decreases by the factor of 2-3 with an increase in swirl intensity as compared to non-swirling jets.

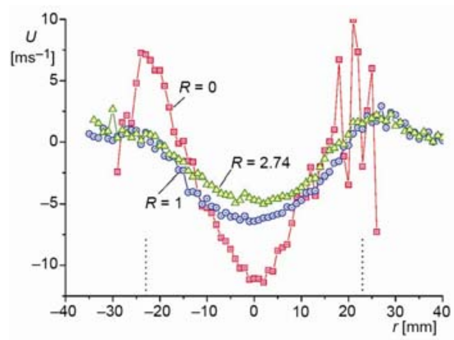

Figure 7. Axial velocity distribution near a dimple, Re = 1.2·10⁴

Distribution of the tangential velocity component and circulation is shown in figs. 8(a) and (b), respectively. These measurements were carried out under the same conditions as the data in fig. 7. Let us make the most important conclusions based on these results. Paradoxically, but with an increase in the initial swirl angle, the maximal value of the tangential velocity component reduces. At this, its maximum increasingly removed from the axis. This feature of the swirl jets is caused by the more intensive process, when mixing at high swirl parameters. Thus, all mentioned peculiarities of hydrodynamics of swirling impinging jets testify previous data on heat transfer regularities.

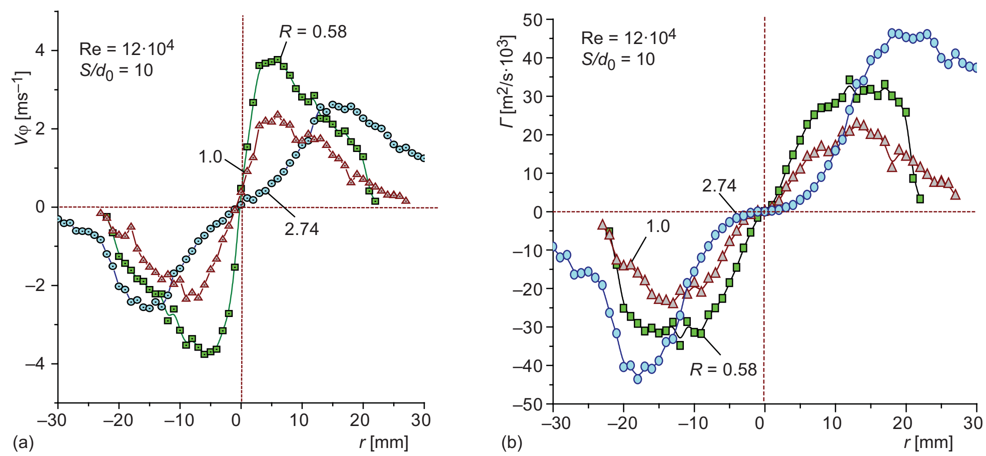

Figure 8. Tangential velocity (a) and circulation (b) distribution near a dimple, Re = $1.2 \cdot 10^4$, S/d_0 = 10

Local and average heat transfer in a dimple

The distribution of local heat-transfer coefficients in the radial direction is shown in fig. 9. The rate of heat transfer is maximal in the absence of jet pre-rotation. As the jet pre-rotation parameter R grows in value, the Nusselt number starts exhibiting a non-monotonic behavior both along the radius, with the formation of additional maxima, and *vs.* R. In the vicinity of the cavity the heat-transfer intensity for swirling jets turns out to be more than twice decreased. On the contrary, in the cavity the heat transfer from the swirling jet turns out to be enhanced in comparison with the case of non-swirling jets, the radial distribution of the heat-transfer coefficient being more uniform here.

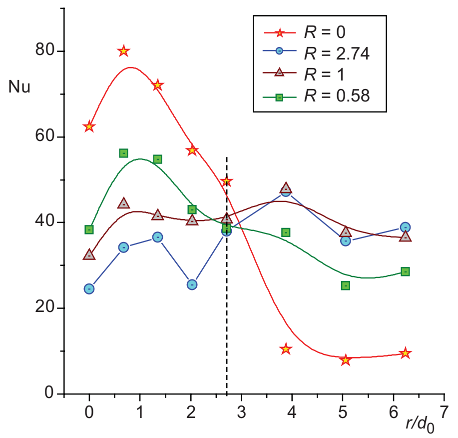

Figure 9. Local heat transfer for an obstacle with spherical cavity impinged by a jet. $Re_0 = 2.8 \cdot 10^4$, $L/d_0 = 10$. The dashed line shows the cavity boundary

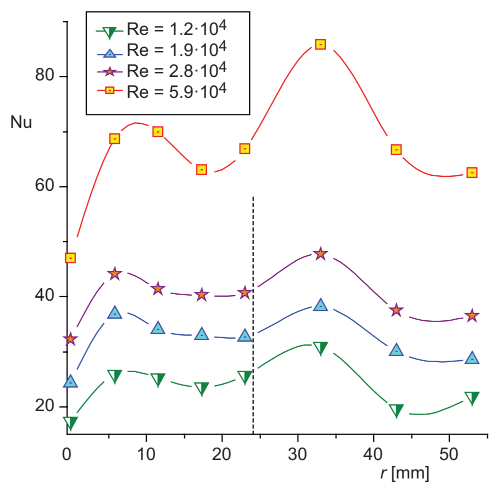

Figure 10. Effect of Reynolds number on the heat transfer of swirling jet, R =1, S/d_0 = 10

The latter points to a greater expansion angle of swirling jets, resulting in a growth of heat transfer in the region outside the cavity.

At fixed jet pre-rotation, the heat-transfer data for different Reynolds numbers proved to be self-similar. This is evident from fig. 10. Only at large Re_d the heat-transfer maxima are pronounced more distinctly, with their position over the radius being quite stable.

An important characteristic of jets impinging onto surfaces is the heat transfer at the stagnation point. The experimental data $Nu_0 = f(Re_0)$ for various jet pre-rotations are shown in fig. 11. Here, the most intense heat transfer is observed in the absence of pre-rotation (R = 0), whereas the increase in the pre-rotation results in that the rate of heat transfer at the center of the cavity decreases. First of all, it is the formation of a complex aerodynamic structure during the interaction of jet with hemispherical cavity that underlies the complex behavior displayed by heat transfer.

From the viewpoint of applications, a most important point in such complex problems is the deduction of correlation dependences for the average heat transfer *vs.* Reynolds number and other governing parameters. In view of axial symmetry, in the present study the average value of the heat-transfer coefficient over the entire surface of cavity was obtained by integrating the local distributions over the radius. The average number $\overline{Nu}_D$ *vs.* Re_0 at $L/d_c = 6$ for various jet pre-rotations is shown in fig. 12. Here, the Nusselt number was calculated from the cavity diameter and from the mean value of the heat-transfer coefficient, $\overline{Nu}_D = \bar{\alpha} D_c / \lambda$. With increasing the jet pre-rotation at all other conditions kept unchanged the heat-transfer intensity decreases in value. For a non-swirling jet, the experimental data obtained at $L/d_0 = 6$ can be fitted with the empirical relation:

$$\overline{Nu}_D = 2.17 \, Re_0^{0.5} \tag{4}$$

typical of laminar heat-transfer mode. As a matter of fact, the flow in the cavity is turbulent. Yet, the specific character of the formed flow pattern, namely, the involvement of reverse flows, curved flow streamlines, large-scale structures, *etc.*, has resulted in the before relation for heat transfer. Apparently, type of relations (4) will undergo changes with distance to the heat-exchanging surface, and for this evolution to be clarified additional tests or numerical experiments are required. Although the rate of heat transfer in the cavity proper decreases in the case of swirling jets, the total heat transfer, including the area adjacent to the cavity may be increased. For this possibility to check, here again additional studies are required.

The influence of a swirl degree on average heat transfer from the entire surface of a hole is obviously shown in fig. 13. It can be seen that at all experimental Reynolds numbers, an increase in the swirl degree reduces heat transfer. This result, surprising at the first glance, as it is shown before, is explained by rapid spreading of the jet due to intensive mixing with the environment. It is obvious that under other boundary conditions, the mixing process will be determined by the specifics of mixing layer formation. Therefore, to determine the general laws of the heat and mass transfer processes, it is necessary to perform the extensive research.

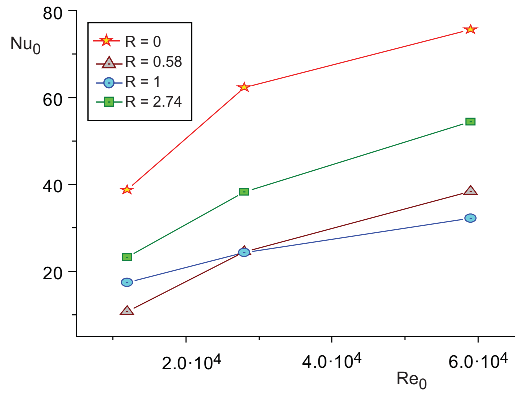

Figure 11. Distribution of Nu_0 at the stagnation point of the flow, $S/d_0 = 10$

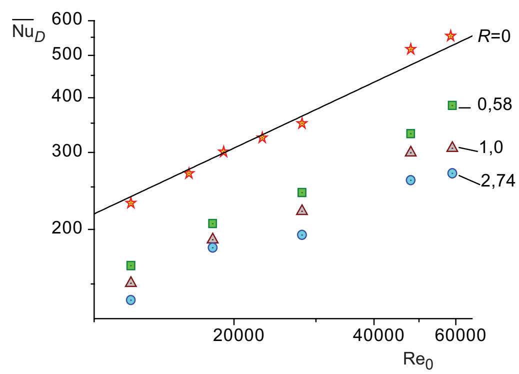

Figure 12. The $\overline{Nu}_D$ averaged over the cavity surface *vs.* jet pre-rotation, $S/d_0 = 6.0$

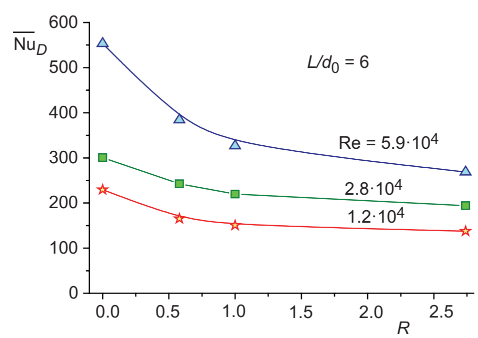

Figure 13. Effect of swirl parameter on average heat transfer over dimple surface

Conclusions

An experimental study of heat transfer during impingement of swirling jet onto hemispherical cavity was performed. It is shown that, following jet pre-rotation, additional maxima appear in the radial distribution of heat transfer, brought about by specific features of mixing processes of eddying jets with ambient air.

The intensity of heat transfer in cavity for swirling jets is substantially, by a factor of 2-3, reduced in comparison with non-swirling jets. On the contrary, outside the cavity the heat transfer for swirling jets is more intense. During variation of jet pre-rotation parameter, the local Nusselt numbers vary non-monotonically both at the stagnant point and at different points over the radius, pointing to a complex mechanism of hydrodynamic and thermal processes in swirling jets impinging onto spherical cavities. At fixed distance to the plate and at jet pre-rotation parameter kept unchanged the distributions of heat transfer are self-similar if considered *vs.* the Reynolds number.

Acknowledgment

This work was supported by the Russian Scientific Foundation (project No. 14-19--00402).

References

[1] Yudaev, B. N., *et al.*, *Heat Transfer in Jet Flows Impinging on Obstacles* (in Russian), Mashinostroenie, Moscow, 1977
[2] Martin, H., Heat and Mass Transfer between Impinging Gas Jet and Solid Surface, *Advances in Heat Transfer,* Vol. 13, Academic Press, New York, USA, 1977
[3] Kanokjaruvijit, K., Martinez-Botas, R. F., Parametric Effects on Heat Transfer of Impingement on Dimpled Surface, *J. Turbomashinery, Trans. ASME*, *127* (2005), 2, pp. 287-296
[4] Kanokjaruvijit, K., Martinez-Botas, R. F., Jet Impingement on a Dimpled Surface with Different Cross--flow Schemes, *Int. J. of Heat and Mass Transfer, 48* (2005), 1, pp. 161-170.
[5] Ekkad, S. V., Kontrovitz, D., Jet Impingement Heat Transfer on Dimpled Target Surfaces, *Int. J. of Heat and Fluid Flow*, *23* (2002), 1, pp. 22-28
[6] Terekhov, V. I., *et al.*, Experimental Study of Flow Structure and Heat Transfer under a Jet Flow Past a Spherical-Cavity Obstacle, *J. of Engineering Physics and Thermophysics, 79* (2006), 4, pp. 657-665
[7] Terekhov, V. I., *et al.*, Impingement of an Impact Jet onto a Spherical Cavity: Flow Structure and Heat Transfer, *Int. J. Heat Mass Transfer*, *52* (2009), 11, pp. 2498-2506
[8] Zhang, D., *et al.*, Flow and Heat Transfer Characteristics of Single Jet Impinging on Dimpled Surface, *J. Heat Transfer*, *58* (2013), S1-2, pp. S18-S28
[9] Hrycak, P., Heat Transfer and Flow Characteristics of Jets Impinging on a Concave Hemispherical Plate, *Proceedings,* 7th Int. Heat Trans. Conf., Munich, Germany, Hemisphere Publ. Corp., Washington, New York, London, Vol. 3, 1982, pp. 357-362
[10] Lee, D. H., *et al.*, The Effect of Concave Surface Curvature on Heat Transfer from a Fully Developed Round Impinging Jet, *Int. J. of Heat and Mass Transfer*, *42* (1999), 13, pp. 2489-2497
[11] Halouane, Y., *et al.*, Turbulent Heat Transfer for Impinging Jet Flowing Inside a Cylindrical Hot Cavity, *Thermal Science, 19* (2015), 1, pp. 141-154
[12] Voropayev, S. I., *et al.*, Evolution of a Confined Turbulent Jet in a Long Cylindrical Cavity: Homogeneous Fluids, *Physics of Fluids*, *23* (2011), 11, p. 115106
[13] Kendil, F. Z., *et al.,* Flow Structures of a Round Jet Evolving into a Cylindrical Cavity, *Int. J. Transport Phenomena*, *11* (2009), 2, pp. 165-183
[14] Chandratilleke, T. T., *et al.,* Heat Transfer and Flow Characteristics of Fluid Jets Impinging on a Surface with Cavities*, J. Enhanced Heat Transfer*, *17* (2010), 3, pp. 223-229
[15] Schwarze, R., *et al.*, Experimental and Numerical Investigations of a Turbulent Round Jet into a Cavity, *Int. J. Heat and Fluid Flow*, *29* (2008), 6, pp. 1688-1698
[16] Kang, H., Tao, W.-Q., Heat and Mass Transfer for Jet Impingement in a Cylindrical Cavity with One End Open to the Ambiant Air, AIAA paper 89-0173, 1989
[17] Braikia, M., *et al.*, Improvement of Thermal Homogenization Using Multiple Swirling Jets, *Thermal Science*, *16* (2012), 1, pp. 239-250.
[18] Ianiro, A., Cardone, G. Heat Transfer Rate and Uniformity in Multichannel Swirling Impinging Jets, *Appl. Thermal Eng., 49* (2012), Dec., pp. 89-98
[19] Zharova, I. K., *et al.*, Investigation of Interaction between Impinging Jet and Surface with Complex Form (in Russian), *Proceedings,* XXIX Siberian Thermophysical Seminar, Novosibirsk, Russia, 2010, pp. 83-94
[20] Singh, S., Chander, S., Heat Transfer Characteristics of Dual Fame with Outer Swirling and Inner Non-Swirling Fame Impinging on a Fat Surface, *Int. J. Heat and Mass Transfer*, *77* (2014), Oct., pp. 995-1007
[21] Zhao, Z., *et al.*, Thermal Performance of a Premixed Impinging Circular Flame Jet Array with Induced-Swirl, *Applied Thermal Engineering 29* (2009), 1, pp. 159–166
[22] Terekhov, V. I., Kalinina, S. V, Flow and Heat Transfer in a Single Spherical Cavity: State of the Problem and Unanswered Questions, *Thermophysics and Aeromechanics*, *9* (2002), pp. 497-520

[23] Afanasyev, V. N., *et al.*, Turbulent Flow, Friction and Heat Transfer Characteristics for Spherical Cavities on a Flat Plate, *Exp. Thermal and Fluid Science*, *7* (1993), 1, pp. 1-8
[24] Terekhov, V. I., *et al.*, Heat-Transfer Coefficient and Aerodynamic Resistance on a Surface with a Single Dimple, *Enhanced Heat Transfer*, *4* (1997), 2, pp. 131-145
[25] Mahmood, G. I., Ligrani P. M., Heat Transfer in a Dimpled Channel: Combined Influences of Aspect Ratio, Temperature Ratio, Reynolds Number, and Flow Structure, *Int. J. Heat Mass Transfer*, *45* (2002), 10, pp. 2011-2020
[26] Ward, J., Mahmood, M., Heat Transfer From a Turbulent Swirling, Impinging Jet, *Proceedings,* 7th Int. Heat Trans. Conf. Munich, Germany, Hemisphere Publ. Corp., Washington, New York, Vol. 3, 1982, pp. 401-406
[27] Lukashov, V. V., *et al.*, The Analysis of Research Results of Heat Transfer Swirled and Non-Swirled Impinging Jets (in Russian), *Izv. SO AN USSR, 6* (1989), pp. 133-142
[28] Volchkov, E. P., *et al.*, Friction and Heat Transfer in a Spatial Boundary Layer Forming by Interaction of a Swirling Flow on a Plane, *Proceedings,* 2nd World Conf. on Exp. Heat Transfer, Fluid Mech. and Thermodynamics, Dubrovnik, Croatia, 1991, pp. 112-117
[29] Huang, B., *et al.*, Heat Transfer under a Laminar, Swirling, Impinging Jet – a Numerical Study, *Proceedings*, 6th Int. Heat Transfer Conf., Toronto, Canada, Vol. 5, 1978, pp. 311-316
[30] Wen, M.-Y., Jang, K.-J., An Impingiment Cooling on a Flat Surface by Using Circular Jet with Longitudinal Swirling Strips, *Int. J. Heat and Mass Transfer*, *46* (2003), 24, pp. 4657-4667
[31] Nozaki, A., *et al.*, Heat Transfer Mechanism of a Swirling Impinging Jet in a Stagnation Region, *Heat Transfer – Asian Research*, *32* (2003), 8, pp. 663-673
[32] Kinsella, C., *et al.*, Heat Transfer Enhancement From a Horizontal Surface by Impinging Swirl Jets, *Proceedings*, 5th European Thermal-Sciences Conference, Eindhoven, The Netherlands, 2008
[33] Felli, M., *et al.*, Distance Effect on the Behavior of an Impinging Jet by PIV and Flow Visualizations, *Exp., in Fluids, 48* (2010), 2, pp. 197-209
[34] Shuja, S. Z., *et al.*, Confined Swirling Jet Impingement onto an Adiabatic Wall, *Int. J. Heat and Mass Transfer, 46* (2003), 16, pp. 2947-2955
[35] Ahmed, Z. U., *et al.*, The Effect of Inflow Conditions on the Development of Non-Swirling Versus Swirling Impinging Turbulent Jets, *Computers & Fluids, 118* (2015), Sep., pp. 255-273
[36] Salman, S. D., *et al.*, Experimental and Numerical Investigations of Heat Transfer Characteristics for Impinging Swirl Flow, *Advances in Mechanical Engineering*, *6* (2014), Aug., pp. 631081-631089
[37] Nuntadusit, C., *et al.*, Visualization of Fow and Heat Transfer Characteristics for Swirling Impinging Jet, *Int. Com. Heat and Mass Transfer, 39* (2012), 5, pp. 640-648
[38] Lee, D. H., *et al.*, Turbulent Heat Transfer From a Flat Surface to a Swirling Round Impinging Jet, *Int. J. Heat and Mass Transfer*, *45* (2002), 1, 223-227
[39] Alekseenko, S. V., *et al.*, Experimental Study of an Impinging Jet with Different Swirl Rates, *Int. J. Heat and Fluid Flow*, *28* (2007), 6, 1340-1359
[40] Ortega-Casanova, J., CFD and Correlations of the Heat Transfer from a Wall at Constant Temperature to an Impinging Swirling Jet, *Int. J. Heat and Mass Transfer*, *55* (2012), 21-22, pp. 5836-5845
[41] Terekhov, V. I., Mshvidobadze, Yu. M., Fluid Flow and Heat Transfer at Interaction Impinging Swirling Jet with a Dimple, *Proceedings,* Int. Conf. on Jets, Wakes and Separated Flows, ICJWSF-2010, Cincinnati, O., USA, 2010
[42] Terekhov, V. I., Mshvidobadze, Yu. M., Aerodynamics and Heat Transfer on Impinging Twisted Jets on Spherical Cavity, *Heat Transfer Res*., *41* (2010), 4, pp. 389-400
[43] Terekhov, V. I., *et al.*, Investigation Into the Flow Structure and Heat Transfer of a Jet Flow Impinging Perpendicularly on a Complex-Geometry Obstacle (in Russian), *Proceedings,* XXVII Siberian Thermophysical Seminar, Novosibirsk, Russia, No.143, 2004
[44] Sapozhnikov, S. Z., *et al.*, *Gradient Heat-Flux Probes* (in Russian), SPTU Press, St.-Petersburg, Russia, 2003

Paper submitted: August 19, 2015
Paper revised: August 20, 2015
Paper accepted: August 27, 2015